Structural Analysis of Novel [60]Fullerene Bisadduct Regioisomers by DFT Calculation

Ken Kokubo[ab]; Sammaiah Thota[a]; Hsing-Lin Wang[c]; Long Y. Chiang[a]

[a] Department of Chemistry, Institute of Nanoscience and Technology, University of Massachusetts Lowell, Lowell, MA [b] Division of Applied Chemistry, Graduate School of Engineering, Osaka University, Suita, Osaka, Japan [c] Chemistry Division, Los Alamos National Laboratory, Physical Chemistry and Spectroscopy Group, Los Alamos, NM

PLEASE SCROLL DOWN FOR ARTICLE

Taylor & Francis
Taylor & Francis Group

Structural Analysis of Novel [60]Fullerene Bisadduct Regioisomers by DFT Calculation

KEN KOKUBO[*,1,2], SAMMAIAH THOTA[1], HSING-LIN WANG[3] and LONG Y. CHIANG[*,1]

[1]*Department of Chemistry, Institute of Nanoscience and Technology, University of Massachusetts Lowell, Lowell, MA 01854*
[2]*Division of Applied Chemistry, Graduate School of Engineering, Osaka University, Suita, Osaka 565-0871, Japan*
[3]*Physical Chemistry and Spectroscopy Group, Chemistry Division, Los Alamos National Laboratory, Los Alamos, NM 87545*

The structural analysis of the first [60]fullerenyl 1,38-bisadduct having the almost perpendicular angle between two addends was performed based on the simulation of ^{13}C-NMR spectral line patterns using the DFT calculation at the B3LYP/6-31G* level of the theory. Among seven closely related model regioisomers of $C_{60}(CH_3)_2$ applied in the calculation, we confirmed that the 1,38-bisadduct and 1,4-bisadduct, being the most plausible regioisomers in a structure showing an approximate consistency of spectral line profiles, match with that of the experimentally obtained spectrum.

Keywords: Fullerene functionalization, [1,6]-addition, bisadduct, DFT calculation, ^{13}C-NMR spectrum pattern, C_s symmetry

1 Introduction

Fullerene derivatives consisting of a limit number of alkyl addends or a low degree of functionalization may maintain the high electronegativity and electron accepting properties of the fullerenyl cage owing to minimum disruption of the spherical π-conjugation system. These main characteristic physical properties of functionalized fullerenes allow their application as a new class of carbon materials in optoelectronic devices. In this viewpoint, a number of fullerene derivative examples with a either 3, 5, or 6 membered cyclic ring attached on the [6,6] bond have been synthesized successfully (1). One of typical examples was given by PCBM (2), which is the most commonly used fullerene derivative as a *n*-type organic semiconductor in photovoltaic, field effect transistor, and photodetector applications (3).

However, the carbon positions at which the acyclic moieties can be attached on a C_{60} is rather limited to satisfy with certain constraints, such as maximizing the aromaticity and minimizing the steric repulsion among addends. In general, [1,2]-addition (4) on [6,6]-bond is energetically favored if the addend is not bulky. With the increasing degree of bulkiness or the addend size, [1,4]-addition (5) on the same ring moiety becomes the preferred reaction route, giving *noncyclized* derivatives.

Recently, we synthesized and characterized a novel [60]fullerene bisadduct $C_{60}[CCH_3(COOEt)_2]_2$ **3a** consisting of two tertiary alkyl addends separated by four fullerenyl carbons in positions arising from the [1,6]-addition reaction to afford the first example of 1,38-bisadduct, as shown in Scheme 1 (6). We regarded this compound as a bisadduct intermediate for the formation of emerald green [60]fullerene hexaadduct EF-6MC$_n$ in the subsequent addition reactions (7). Although we were able to grow a single-crystal of EF-6MC$_n$ and had its structure determined by the X-ray single-crystal structural analysis, our extensive attempts to form a single crystal of the bisadduct **3a** under various experimental conditions were not successful. Accordingly, we applied ^{13}C-NMR spectroscopic simulation of several possible bisadduct regioisomers for the comparison with that of the product **3a** obtained. In this paper, we report the fully structural analyses of the first 1,38-bisadduct **3a**, showing a respective perpendicular (90°) angle arrangement between two 2-methyl-diethylmalonate addends, based on
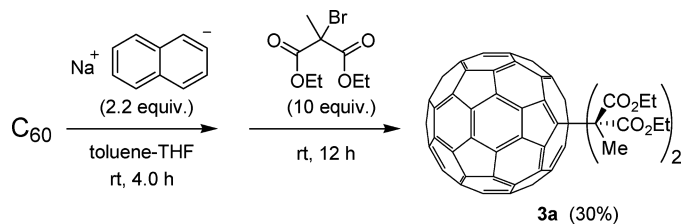
Sch. 1. Synthesis of the 1,38-bisadduct $C_{60}[CMe(CO_2Et)_2]_2$ **3a** by dianionization reaction of C_{60} with sodium naphthalenide, followed by quenching with 2-bromo-2-methyl-diethyllmalonate.

the simulation of the ^{13}C-NMR spectral line pattern using the DFT calculation at the B3LYP/6-31G* level of the theory.

2 Experimental

2.1 General and Instrumentation

All reagents and solvents were purchased from Aldrich or Fischer and used as received. NMR spectra were recorded on a Bruker-400 spectrometer in CDCl$_3$ and referenced to CDCl$_3$. UV−Vis spectra were measured using a Varian Cary 500 UV−Vis−NIR spectrophotometer.

2.2 Geometry Optimization and ^{13}C-NMR Spectra Prediction

All calculations were performed using the Spartan 06 software. Geometries were optimized using the density functional theory (DFT) with the B3LYP functional level and the 6-31G* basis set (B3LYP/6-31G*).

2.3 Synthesis of 1,38-bisadduct $C_{60}[CMe(CO_2Et)_2]_2$ 3a

A two-neck round bottle flask (100 ml) containing naphthalene (78 mg, 0.61 mmol) and sodium metal (14 mg, 0.061 mmol) was evacuated and repeatedly purged with nitrogen gas three times. Freshly distilled dry THF (100 ml) was added to the flask via syringes and stirred at room temperature until the solution color changed to dark green (about 4.0 h). The resulting dark green sodium-naphthalenide solution was injected slowly into the deoxygenated solution of C_{60} (200 mg, 0.28 mmol) in toluene (100 ml). The mixture was allowed to stir for a period of 4.0 h at room temperature, followed by the addition of diethyl 2-bromo-2-methyl-diethylmalonate (708 mg, 2.78 mmol). It was stirred for an additional 12 h at room temperature. During the work up, the solvent was evaporated under reduced pressure, and the residue was purified on a silica gel column using toluene−THF (98:2) as eluent to afford the desired product 1,38-bis(2-(2-methyl-diethylmalonyl))[60]fullerene $C_{60}[CMe(CO_2Et)_2]_2$ **3a** (88 mg, 30% yield). Mp >200°C (decomposed); ^{1}H NMR (400 MHz, CDCl$_3$) δ 4.35 (q,

8H), 2.45 (s, 6H), and 1.32 (t, 12H); ^{13}C NMR (100 MHz, CDCl$_3$) δ 170.00 (C=O), 169.85 (C=O), 153.77 (2C), 151.50 (2C), 148.68 (2C), 148.37 (2C), 147.27 (2C), 147.07 (2C), 146.93 (2C), 146.73 (2C), 145.86 (2C), 145.78 (2C), 145.54 (2C), 145.15 (2C), 144.79 (2C), 144.44 (2C), 144.18 (1C), 144.13 (2C), 143.85 (2C), 143.79 (2C), 143.30 (2C), 143.11 (4C), 143.02 (2C), 142.82 (1C), 142.68 (1C), 142.64 (2C), 142.57 (2C), 142.51 (2C), 141.06 (2C), 140.14 (1C), 138.16 (2C), 137.68 (2C), 62.23 (2C), 62.14 (2C), 60.43 (2C), 20.96 (2C), and 14.08 (4C).

3 Results and Discussion

The reaction of dianionic C_{60} (C_{60}^{2-}) with 2-bromo-2-methylmalonate using sodium naphthalenide as the electron reducing agent was carried out by the procedure reported previously (Scheme 1) (6). The structure of the major product 1,38-bis(2-(2-methyl-diethylmalonyl))[60]fullerene as the 1,38-bisadduct **3a**, isolated and purified via thin-layer chromatography (TLC) as shown in Figure 1, was characterized using various spectroscopic methods, including the analyses of ^{1}H and ^{13}C-NMR, MALDI-TOF mass, and UV−Vis spectra. Due to the significant bulkiness of the tertiary substituent moiety $-CMe(CO_2Et)_2$ on the cage surface, it is unlikely for the proceeding of [1,2]- and, probably, the [1,4]-addition reactions to occur that resulted in the corresponding structure of **3g** and **3f**, respectively. ^{13}C-NMR spectrum of **3a** displayed 30 carbon signals including 4 peaks in a half-intensity with respect to the others in the chemical shift range of δ 138−154 that can be accounted for the fullerenyl sp^2 carbons (Fig. 2, top). This spectral pattern fits well with a structure of [60]fullerene bisadduct having a C_S symmetry. Accordingly, we conducted the ^{13}C-NMR spectral simulation of four possible model bisadduct compounds $C_{60}(CH_3)_2$ **1a−d** exhibiting a C_S symmetry as an approach of making the spectral correlation to that of $C_{60}[CMe(CO_2Et)_2]_2$ **3a**, along with C_2-symmetrical $C_{60}(CH_3)_2$ **1e** for the comparison, using the DFT calculation at the B3LYP/6-31G* level of theory. The fullerenyl carbon positions bearing an alkyl addend in the structure of these regioisomers are numbered according to the IUPAC rule for [60-I_h] fullerene, generally written as C_{60}, using a Schlegel diagram (Fig. 1).

The calculated ^{13}C-NMR spectral line patterns for the isomers **1a−e** were shown in Figure 2. Due to the lack of a solvent parameter and the limitation of the calculation accuracy, chemical shifts of fullerenyl sp^2 carbons in **1a−e** were slightly shifted to upfield and significantly to downfield in the full range of δ 130−170 with the obvious broadening of the spectral width as compared with the experimental range. Although such a difference in the chemical shift was observed, in principle, the simulated spectral line patterns should show useful information to assess the structure. In the case of C_S-symmetrical isomers **1a−d**, four
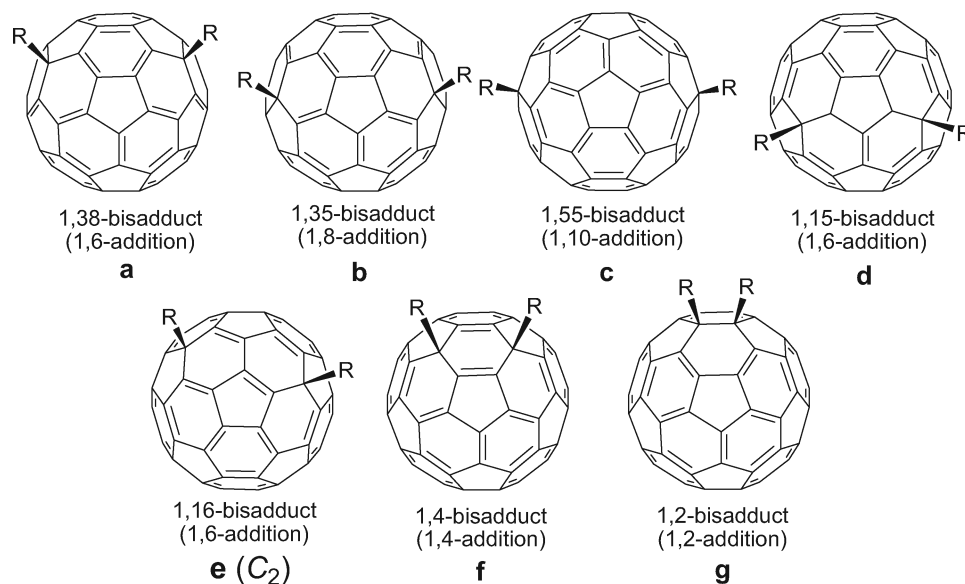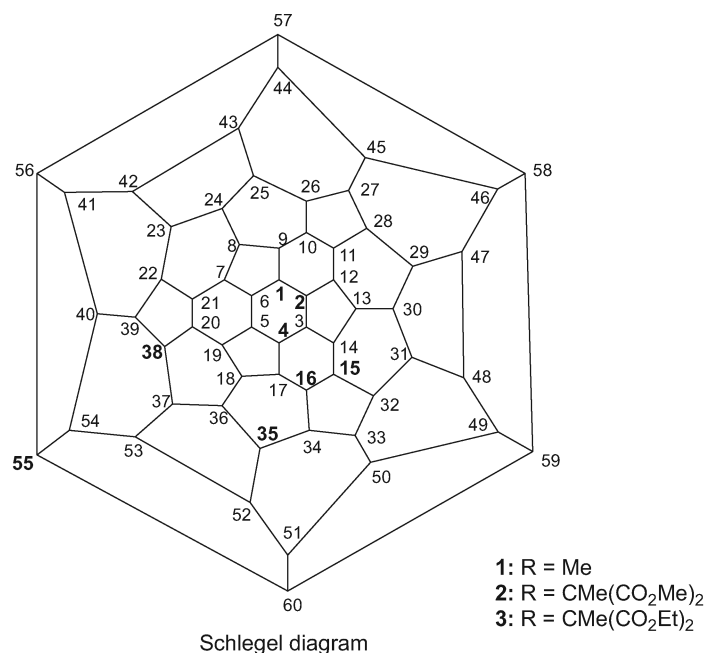
Schlegel diagram

1: R = Me
2: R = CMe(CO$_2$Me)$_2$
3: R = CMe(CO$_2$Et)$_2$

1,38-bisadduct
(1,6-addition)
a

1,35-bisadduct
(1,8-addition)
b

1,55-bisadduct
(1,10-addition)
c

1,15-bisadduct
(1,6-addition)
d

1,16-bisadduct
(1,6-addition)
e (*C$_2$*)

1,4-bisadduct
(1,4-addition)
f

1,2-bisadduct
(1,2-addition)
g

Fig. 1. The IUPAC numbering rule for [60-*I*$_h$]fullerene (C$_{60}$) and the plausible bisadducts derived from the reaction of C$_{60}$ with 2-bromo-2-methylmalonate (*C*$_S$ symmetry except for **e**). DFT calculations were performed for **1a–e** as model compounds.

simulated peaks each in a half-intensity, corresponding to the carbons located on the mirror plane, were observed even though certain peak overlap with other peaks may occur. Contrarily, the regioisomer **1e** does not show any half-intensity peak since no mirror symmetry plane possible for the *C$_2$* symmetrical structure. As for the highly symmetrical isomer **1c**, the number of peaks was obviously fewer than those of other isomers. In fact, in the structure of **1c**, a second mirror plane exists that dissects through both two CH$_3$-attached fullerenyl carbons and changes its molecular symmetry from *C$_s$* to *C$_{2v}$*. Among the rest of

isomers **1a**, **1b**, and **1d** arising from either the [1,6]- or [1,8]-addition reaction, ^{13}C NMR spectral pattern profile of **1a** bears a close resemblance to that of the experimental data. Some correlated peak line features were indicated by arrows in Figure 2 to demonstrate the degree of resemblance between that of **1a** and the experimental spectrum.

While the distance between two CH$_3$-attached fullerenyl sp^3 carbons in **1a**, **1b**, and **1d** is almost in the similar range of ~5.0 to 6.0 Å, the interspacing bond angles between these two methyl groups, defined as the positional angles here, were slightly different from each other in a decreasing

Table 1. ^{13}C-NMR pattern matching between calculated spectra and experimental ones along with calculated values for the relative heat of formation ΔH_f and the positional angle

Regioisomers	*1a*	*1b*	*1c*	*1d*	*1e*	*1f*	*1g*
^{13}C NMR Pattern[a]	good	fair	different	fair	different	fair	–
Position distance[b]/Å	5.64	6.55	7.53	5.07	5.23	3.09	1.62
Positional angle[c]/°	94.6	117.4	158.8	83.0	85.9	48.4	45.7
$\Delta\Delta H_f{}^d$/kJmol^{-1}	0	−43.6	−10.1	+1.39	−67.2	−111.8	−119.9
Number of C=C in five-membered ring	6	3	5	4	2	1	0

[a]Compared with the experimental spectrum; [b]The distance between two carbons adjacent to the methyl group; [c]The angle between two methyl groups; [d]The heat of formation relative to the isomer **1a**.

order of **1b** (117°) > **1a** (95°) > **1d** (83°), as shown in Table 1. By taking the same positional angle between any two addends in the structure of emerald green [60]fullerene hexaadduct EF-6MC$_n$ as the reference, it was confirmed as a 90° in the perpendicular position to each other by its X-ray single crystal structural analysis, leading to a highly symmetrical D_3 structure (7). Therefore, it is perceptible for us to propose that the most likely intermediate bisadduct

formation in the process of a sequential reaction mechanism leading to the formation of EF-6MC$_n$ should consist of two methyl groups following the same positional angle around 90°. In fact, it was found to be the case for **1a**. Based on the Schlegel scheme of the EF-6MC$_n$ hexaadduct (7), two isomeric possibilities for the intermediate bisadduct can be revealed; the first isomer as **1a** with a C_s symmetry and the second isomer as **1e** with a C_2 symmetry. This
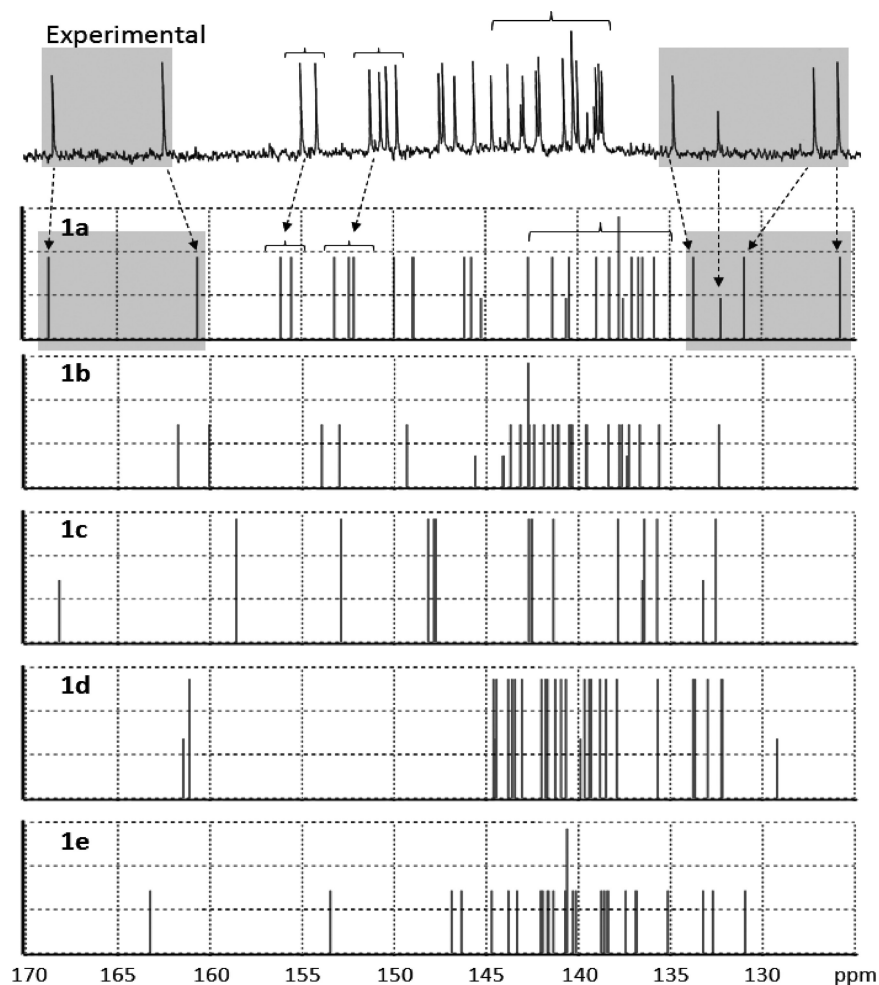
Fig. 2. Simulated ^{13}C-NMR spectral line pattern for regioisomers **1a–e** and their comparison with the experimentally obtained spectral data.

structural elucidation is well consistent with the result of the ^{13}C-NMR simulation.

Other interesting feature concerning with this plausible bisadduct **1a** is its thermodynamic instability. Calculated values of the heat of formation $\Delta\Delta H_f$ relative to **1a** were summarized in Table 1. Despite of the limit steric hindrance of the addend (–CH$_3$ in this model case), $\Delta\Delta H_f$ was found to increase roughly proportional to the increase of the distance between the methyl groups in the order of 1,2-addition **1g** (position distance of 1.62 Å) < 1,4-addition **1f** (3.09 Å) < 1,6-addition **1e** (5.23 Å) < 1,8-addition **1b** (6.55 Å). Therefore, the stability is obviously not determined by the steric hindrance but rather by certain electronic factors which may be related to the expansion of π-conjugation length and the cage strain. It is well known that a C$_{60}$ derivative containing a less number of double bonds in the pentagon ring moiety is more energetically favorable (8). Interestingly, tendency of the DFT calculation data obtained was well consistent with this rule. Basically, the stability may decrease upon the increasing number of double bonds, roughly in the order of **1g** (the number of C=C in one pentagon = 0; $\Delta\Delta H_f = -120$ kJ/mol) < **1f** (1; −112) < **1e** (2; −67) < **1b** (3; −44) < **1d** (4; +1.4) ≈ **1c** (5; −10) < **1a** (6; 0). Accordingly, the plausible 1,38-bisadducts **1a** and **3a** are not formed thermodynamically. If the size of the addend becomes larger going from −CH$_3$ to −CMe(CO$_2$Et)$_2$, the energy gap of ΔH_f between **3g** and **3a** [–CMe(CO$_2$Et)$_2$] may turn into less than the value of that between **1g** and **1a** (−CH$_3$) owing to the increased steric repulsion. Neverthe-

less, it is notable that such a thermodynamically unstable isomer **3a** can be the major isomeric product if the kinetic control plays a significant role in the reaction process. This selectivity clearly excludes the rearrangement or trotting of the addends on the C$_{60}$ cage surface (9), which may result in the formation of more thermodynamically favorable regioisomers, under the present reaction conditions.

In Figure 3, all ^{13}C chemical shift values calculated for **1a** were plotted and indicated on the 3D model. Although it is rather difficult to find clear rules for the correlation between the position and the chemical shift, three carbon lines at the downfield region over δ 160 were found to locate closely to the methyl group. In fact, two of them were just adjacent to the CH$_3$-attached fullerenyl sp^3 carbon on a [5,6]-bond. Such a downfield shift may be induced by the high strain and destabilization around the fullerenyl sp^3 carbon region (10). This large strain energy may partly reflect the higher ΔH_f value of **1a**.

A chemical shift could also be influenced by the electronic nature of the addend through the magnetic shielding effect. Accordingly, the control DFT simulation was also conducted for the ^{13}C-NMR spectrum in the case of **2a**, which has the similar functional diester moiety of –CMe(CO$_2$Me)$_2$ to the experimental product **3a**. Indeed, the upfield shift of several carbon peak lines in the downfield region (δ 169 → 163) was observed as compared with the spectrum of **1a** (Fig. 4). Even though it is apparently difficult to explain all these observations, however, the range of chemical shift values of **2a** was better fitted in line with the experimental value of **1a**. Comparison of chemical shift values of the 1,4-bisadduct **1f**, which was a common isomer in other reaction systems, was also carried out with those of **1a** and **2a** (Fig. 4). Due to the less strain energy ($\Delta\Delta H_f$ of **1f** is very low as −111.8 kcal/mol), the significant upfield shift of the carbon peak lines in the downfield region (δ 169 → 157) was observed. Despite the values being quite similar to the experimental ones, the spectral line pattern was rather fair. In the absence of the X-ray single crystal structural analysis to confirm the precise structure of the bisadduct **3a**, certain uncertainty arguments do exist
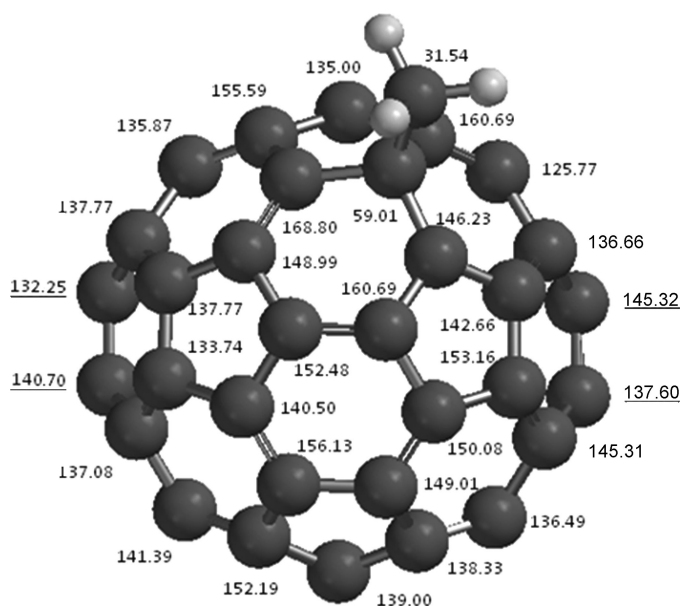

Fig. 3. Calculated chemical shifts of ^{13}C NMR spectrum for the 1,38-bisadduct **1a**. Only a hemisphere divided by the symmetrical mirror plane σ_v is shown for clarity. Chemical shift of four carbons underlined in value, each corresponding to a peak in half intensity with respect to the others, in ^{13}C-NMR spectrum are located on the mirror plane.
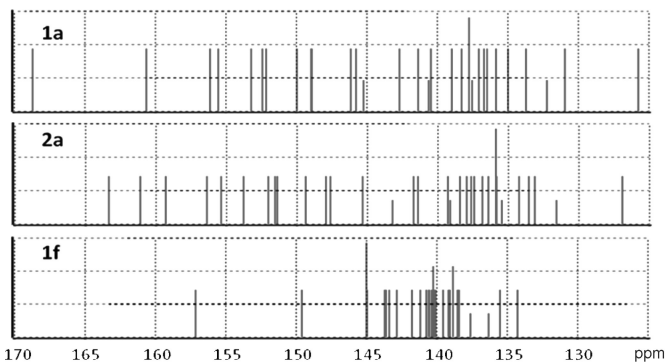

Fig. 4. Comparison of calculated ^{13}C NMR spectral line patterns between three regioisomers **1a**, **2a**, and **1f**.

over its regioselectivity. Therefore, the present simulation results based on DFT calculations should provide valuable insights into these arguments.

4 Conclusions

In conclusion, we performed extensive, simulative estimation of the ^{13}C-NMR spectral line patterns using the DFT calculation at the B3LYP/6-31G* level of the theory on seven closely related model regioisomers in a molecular formula of $C_{60}(CH_3)_2$ **1a−g**. As a result, the most plausible regioisomers were found to be a novel 1,38-bisadduct **1a** and a 1,4-bisadduct **1f** showing an approximate consistency of spectral line profiles in matching with that of the experimentally obtained spectrum of **3a**.

Acknowledgement

References

1. Hirsch, A. and Brettreich, M. *Fullerenes, Chemistry and Reactions*, Wiley-VCH: Weinheim, Germany, 2005.
2. Kim, J.Y., Lee, K., Coates, N.E., Moses, D., Nguyen, T.-Q., Dante, M. and Heeger, A.J. (2007) *Science*, 317, 222.
3. Kronholm, D. and Hummelen, J.C. (2007) *Materials Matters*, 2, 16.
4. (a) Henderson, C.C. (1993) *Science*, 259, 1885; (b) Caron, C. (1993) *J. Am. Chem. Soc.*, 115, 8505; (c) Hirsch, A. (1993) *Chem. Ber.*, 126, 1061; (d) Boltalina, O.V. (2000) *Chem. Commun.*, 1601; (e) Meier, M.S. (2001) *Org. Lett.*, 3, 1717.
5. (a) Wang, G.-Wu., Murata, Y., Komatsu, K. and Wan, T.S.M. (1996) *Chem. Commun.*, 2059; (b) Birkett, P.R. (1997) *J. Chem. Soc., Perkin Trans.*, 2, 457.
6. Wang, C.-C.; Gao, Y., Kokubo, K., Chiang, L.Y. and Wang, H.-L. In communication.
7. (a) Canteenwala, T., Padmawar, P.A. and Chiang, L.Y. (2005) *J. Am. Chem. Soc.*, 127, 26; (b) Canteenwala, T., Li, W., Wang, H.L. and Chiang, L.Y. (2006) *Chem. Lett.*, 35, 762.
8. Wang, B.-C. and Cheng, C.-Y. (1997) *J. Mol. Struct. (Theochem)*, 391, 179.
9. Miller, G.P., Millar, J.M., Liang, B., Uldrich, S. and Johnston, J.E. (1993) *J. Chem. Soc., Chem. Commun.* 893.
10. Avent, A.G., Darwish, A.D., Heimbach, D.K., Kroto, H.W., Meidine, M.F., Parsons, J. P., Remars, C., Roers, R., Ohashi, O., Taylor, R. and Walton, D.R.M. (1994) *J. Chem. Soc., Perkin Trans.* 2, 15.